Available online at www.sciencedirect.com
ScienceDirect
Polymer 48 (2007) 2071–2078
polymer
www.elsevier.com/locate/polymer

Plasma-induced polymerisation of hydrophilic coatings onto macroporous hydrophobic scaffolds

A. Serrano Aroca [a,*], M. Monleón Pradas [a,b], J.L. Gómez Ribelles [a,b]

[a] *Center for Biomaterials, Universidad Politécnica de Valencia, Camino de Vera s/n, 46022 Valencia, Spain*
[b] *Centro de Investigación Príncipe Felipe, Avda. Autopista del Saler 16, 46013 Valencia, Spain*

Received 14 July 2006; received in revised form 25 January 2007; accepted 9 February 2007
Available online 14 February 2007

Abstract

Macroporous poly(methyl methacrylate) scaffolds with a well-interconnected pore architecture were coated with poly(2-hydroxyethyl acrylate) following a particular protocol of plasma-induced polymerisation. Plasma-polymerised PHEA (*pl*PHEA) was grafted onto two macroporous poly(methyl methacrylate) scaffolds with varying cross-linking density showing significant differences in the interpenetration of the coating and the PMMA substrate. Fourier transform infrared spectroscopy (FTIR) and scanning electron microscopy (SEM) proved that the surface of the pore structure in the whole volume of the sample was coated. The stability of the *pl*PHEA coating was studied by extraction with distilled water at different temperatures. After the extraction, these samples were observed by SEM and analysed by differential scanning calorimetry (DSC) and FTIR showing that only in very drastic conditions *pl*PHEA suffers hydrolytic degradation.

Keywords: Plasma-induced polymerisation; Hydrogel; Water sorption

1. Introduction

Many macroporous polymers are under research to be employed as scaffolds or three-dimensional porous matrices in tissue engineering [1–5]. Their design characteristics are major challenges for the field, and should be considered at a molecular chemical level. Scaffold materials must have a highly porous structure with a high surface/volume ratio to allow cell attachment.

The combination of the adequate mechanical properties to sustain the forces to which the scaffold is subjected *in vivo* and the surface characteristics to facilitate cell attachment is sometimes difficult. The surface modification through grafting on the macroporous polymeric substrate may be a solution, provided the coating penetrates in the whole pore structure and the porosity is not affected. Plasma surface modification or coating by plasma polymerisation is an interesting approach in this line.

Plasma contains activated species, electrons, ions and radicals, which able to initiate chemical or physical reactions at the solid surface of polymers. As a result, modification reactions at the surface occur and cause alteration of surface properties and surface morphology. The reaction initiated by these species depends mainly on the nature of the plasma gases as well as the energy level of the plasma and nature of the polymeric materials. The plasma composed of inorganic gases such as argon, helium, hydrogen, nitrogen, and oxygen leads to implantation of atoms, radical generation, and etching reactions. This is the case of a novel ammonia plasma treatment protocol developed to achieve the effective through-thickness modification of large porous scaffolds [6]. Nevertheless, when plasma interacts with organic molecules in a vapour phase, polymerisation may take place, and all surfaces of substrates inside the plasma chamber are coated with the polymers formed. This process is called *plasma polymerisation* [7,8] and the product obtained is *plasma polymer*. Plasma is an

* Corresponding author. Tel.: +34 963877007x88930; fax: +34 963877276.
E-mail address: anserar@ter.upv.es (A. Serrano Aroca).

0032-3861/$ - see front matter © 2007 Elsevier Ltd. All rights reserved.
doi:10.1016/j.polymer.2007.02.017

initiator of these processes and the interaction with plasma plays an important role.

The polymer properties of the plasma polymers are strongly dependent on the plasma conditions (power, gas flow rates, time of treatment and base pressure in the reaction chamber). The concept of the atomic polymerisation points out that elemental reactions occurring in plasma polymerisation are the fragmentation of monomer molecules, the formation of active sites (radicals), and recombination of the activated fragments. If fragmentation and recombination operate in plasma, starting molecules for plasma polymerisation will not be restricted to unsaturated compounds such as vinyl compounds, and saturated compounds can also deposit polymers. Plasma polymers are different in chemical composition from conventional polymers polymerised via radical and ionic reactions, even if the same monomers are used in the two kinds of polymerisation. This is a distinguishing feature of plasma polymerisation. Plasma polymers are not composed of repeating monomer units, but have complicated units containing cross-linked units and units fragmented or rearranged from the monomers. Therefore, plasma polymers are expected to be essentially different in chemical and mechanical properties than conventional ones. The water sorption properties of hydrophilic plasma polymers are also different from the corresponding hydrogels prepared by conventional polymerisation reactions [9,10]. In addition, it is well known that plasma polymers are always cross-linked to some extent [7,11] and for this reason they generally exhibit superior stability to chemical, thermal, and mechanical stress than conventional polymers. Their partial or total insolubility has made plasma polymers rather difficult to characterise.

Plasma polymerisation is usually a thin film-forming process, where thin films deposit directly on surfaces of the substrates [7,8,12]. Various plasma polymer deposition methods are discussed in Ref. [13]. In this work, a different plasma polymerisation method was used in which polymerisation of 2-hydroxyethyl acrylate monomer previously adsorbed on the surface of macroporous PMMA is initiated by the plasma, what can be called *plasma-induced polymerisation*, according to Yashuda [14].

2. Experimental

2.1. Materials and plasma-induced polymerisation

Macroporous PMMA was synthesised by polymerisation in the presence of 70 wt.% of ethanol. The polymerisation took place under UV light with 0.2 wt.% of benzoin (from Scharlau 98% pure) as photoinitiator and 1 or 5 wt.% of ethylene glycol dimethacrylate (EGDMA, from Aldrich 98% pure) as cross-linker. The monomer (methyl methacrylate, MMA, from Aldrich 99% pure) and the cross-linking agent were purified by vacuum distillation. Hereafter these samples will be called as PMMA1/70 and PMMA5/70. Bulk PMMA (non-porous) with different cross-linking densities was synthesised starting from a mixture of MMA and EGDMA monomers in 99/1 and 95/5 weight ratios, which will be called hereafter as PMMAB1 and PMMAB5. Bulk poly(2-hydroxyethyl acrylate) (PHEA) was polymerised under UV light for 24 h with 0.2 wt.% of benzoin as photoinitiator between glass plates to form sheets of approximately 1 mm thick. All the samples were washed with boiling water for 24 h and dried at 90 °C in vacuo for 3 days.

Poly(2-hydroxyethyl acrylate) hydrophilic coatings were grafted onto macroporous PMMA. Macroporous PMMA was allowed to adsorb 2-hydroxyethyl acrylate monomer vapour before plasma treatment. The sample was placed inside a vacuum desiccator on a grid located on the top of a glass with liquid HEA monomer. The air was evacuated from the desiccator with the help of a vacuum pump. After that, this desiccator was placed inside an oven at 50 °C in order to accelerate the adsorption process. Once the samples had adsorbed the desired amount of monomer vapour, they were removed from the desiccator to be treated by plasma right after. The plasma treatment was performed in a Piccolo apparatus from Plasma-electronic GmbH (Germany), which has a stainless steel vacuum chamber with a volume of 45 l. Plasma was generated by a 2.45 GHz Gigatron® device for low-pressure plasmas [15]. The process started with the evacuation of the air present inside the chamber till a base pressure of 50 Pa was achieved. After 5 s of homogenisation, the plasma was generated in the residual air at 50 Pa and 360 W for 110 s. The samples were located approximately at a radial distance of 100 mm from the plasma source. The plasma treatment allowed the adsorbed HEA monomer to polymerise onto the macroporous PMMA scaffold. Finally, the chamber was ventilated to atmospheric pressure in 30 s. Controlling the adsorption time of monomer vapour it was possible to synthesise macroporous PMMA with different fractions of *pl*PHEA (2.8, 11.4, 18.2 and 35.3 wt.% in the case of PMMA polymerised with 1% EGDMA and 25.3 and 55.2 wt.% in the case of PMMA substrates polymerised with 5% EGDMA). The *pl*PHEA concentrations were gravimetrically determined from the mass (in the dry state) of the samples before the monomer vapour adsorption and after the plasma treatment. In both cases, the samples were dried at a temperature higher than T_g in vacuo for 3 days (to constant weight). Hereafter these samples will be designated generically by the name PMMA-*gr*-*pl*PHEA and a particular sample will be designed by the name of the respective porous PMMA followed by -*gr*-*pl*PHEA (wt.%).

A PMMA1/70E (without adsorbing any HEA vapour) was subjected to a plasma treatment with the same plasma process conditions described above in order to discard any effect of the plasma treatment on the morphology of macroporous PMMA.

2.2. Specific volumes

A Mettler Toledo AX205 balance with a sensitivity of 0.01 mg with density accessory kit was used to measure the specific volume of bulk PHEA through the weight of a sample in air and immersed in *n*-octane at 25 ± 0.5 °C. In the case of bulk polymers, the result obtained for a series of pieces of the same sample was reproducible within ±0.002 cm^3/g.

An apparent specific volume (v_{app}) of the porous polymers was calculated from measurements of the three linear dimensions of prismatic samples (approximate dimensions: 10 × 5 × 2 mm) and their weight. The uncertainty of such measurements was estimated by the standard deviation of the values obtained in four pieces of each porous polymer.

2.3. Microscopy

Scanning electron micrographs (SEM) were taken in an ISIDS-130 microscope at an accelerating voltage ranging from 15 to 20 kV. The cryogenic fractures of the samples were sputtered with gold prior to observation.

2.4. Fourier transform infrared spectroscopy (FTIR)

The FTIR spectra shown in this work were taken with a Thermo Nicolet NEXUS spectrometer in the wavenumber region between 400 and 4000 cm^{-1} at room temperature. All measurements were performed by attenuated total reflectance spectroscopy (ATR) with the Smart Mullti-Bounce HATR accessory for solids with a ZnSe crystal. The spectra shown in this work were the result of 32 scans at the speed of 1 scan per second.

2.5. Stability of the *pl*PHEA coating

In order to study the stability of our *pl*PHEA coating grafted onto macroporous PMMA, four kinds of PMMA-*gr*-*pl*PHEA samples were subjected to extraction in distilled water at 25, 50 and 100 °C (boiling water) for 10 days, changing the water every day. Before the immersion in water, the air present in the samples was extracted with a vacuum pump to ensure complete filling of the pores. At the end of the experiment, the samples were dried at 90 °C in vacuo for 3 days (to constant weight) to determine the weight loss. These samples after the extraction with water were analysed by differential scanning calorimetry (DSC) and observed by SEM.

2.6. Differential scanning calorimetry

Differential scanning calorimetry experiments were performed in a Perkin–Elmer (Pyris 1) apparatus. The temperature of the calorimeter was calibrated with water, cyclohexane and *n*-octadecane. The melting heat of indium was used to calibrate the heat flow output. DSC measurements were performed on dry samples. The glass transition temperature was taken from the inflexion point of the heating scan.

2.7. Equilibrium water uptakes

Equilibrium water sorption uptakes were measured at 50 °C. The samples were allowed to equilibrate to constant weight (weight change less than 10^{-4} g) in various desiccators where the relative humidity (rh) was maintained at 0.5093 and 0.9582 using two saturated salt solutions (NaBr and K_2SO_4, respectively) [16]. The water content (w), defined as *g water/g dry sample*, was determined by weighing.

3. Results

3.1. Specific volume and porosity

The specific volume of the bulk polymers at 25 °C ± 0.5 (v_b), the apparent specific volumes of the porous polymers at 25 °C ± 0.5 (v) and the porosities in the dry state before (P_{ref}) and after (P_d) the *pl*PHEA grafting determined from the apparent specific volumes are shown in Table 1.

The porosity of the dry porous polymers ($P_d = V_{pores}/V$) was determined from their apparent specific volumes ($v_{app} = (V_{pores}+V_b)/m_b$) where V_b and m_b are the volume and the mass of the bulk polymers, and the specific volumes of the same bulk polymers as

$$P_d = \frac{v_{app} - v_b}{v_{app}} \quad (1)$$

3.2. Microscopy

By means of scanning electron microscopy (SEM), it is possible to observe the formation of the hydrophilic coating on the macroporous scaffold after the plasma-induced polymerisation. Fig. 1 shows the SEM micrographs of the PMMA1/70E scaffold before and after the plasma grafting. The scaffold consists of adhered PMMA spheres formed by phase separation during the polymerisation in the presence of ethanol (macrosyneresis [17,18]). The influence of the polymerisation conditions on the particle size and the properties of the scaffold has been published elsewhere [19]. The SEM microphotograph of the same sample after a plasma treatment with the same plasma process conditions showed no visual changes in the surface of the PMMA particles (figure not shown). Fig. 1b–e shows the scaffolds after grafting with different wt.% of plasma-polymerised PHEA. The microphotograph corresponding to the sample containing 2.8 wt.% of *pl*PHEA (Fig. 1b) shows some superficial changes with respect to the PMMA scaffold. From 11.4 wt.% *pl*PHEA, a clear homogeneous hydrophilic layer is observed around all the PMMA microspheres. The thickness of the *pl*PHEA layer seems to increase more and more with increasing of the *pl*PHEA content.

Table 1
Specific volumes of the bulk polymers and apparent specific volumes of the porous composites at 25 °C ± 0.5 (v)

Sample	v (cm^3/g)	P_d (%)	P_{ref} (%)
PHEA	0.754 ± 0.002	–	–
PMMAB1	0.862 ± 0.002	–	–
PMMAB5	0.858 ± 0.002	–	–
PMMA1/70E-*gr*-*pl*PHEA (18.2%)	2.142 ± 0.221	61	70
PMMA1/70E-*gr*-*pl*PHEA (35.3%)	2.261 ± 0.041	64	70
PMMA5/70E-*gr*-*pl*PHEA (25.3%)	3.294 ± 0.048	75	76
PMMA5/70E-*gr*-*pl*PHEA (55.2%)	3.031 ± 0.026	74	76

Porosities of the PMMA networks with *pl*PHEA (P_d) and without *pl*PHEA (P_{ref}) in the dry state.

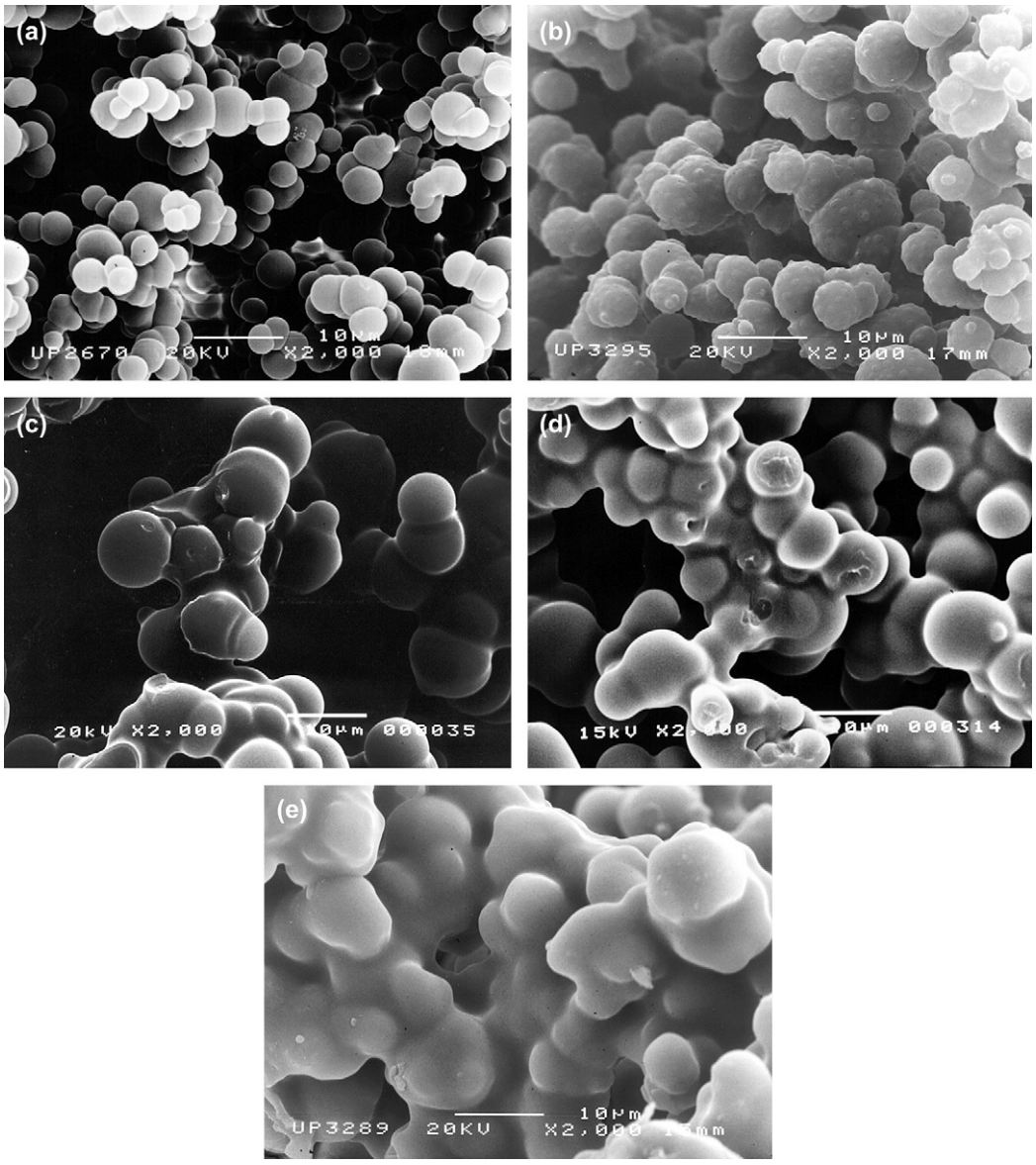

Fig. 1. SEM micrographs of PMMA1/70E treated with plasma for 110 s at 360 W (b) and with different wt.% of plasma-polymerised PHEA (0 (a), 2.8 (c), 11.4 (d), 18.2 (e) and 35.3 (f)) obtained by controlling adsorption time (0 (a), 1.5 (c), 18 (d), 40 (e) and 360 (f) hours, respectively). All micrographs have the same magnification (2000×).

The different morphology is obtained when *pl*PHEA is grafted onto macroporous PMMA with higher cross-linker content can be observed in Fig. 2. PMMA5/70E after the plasma grafting is shown with two different *pl*PHEA contents (25.3 and 55.2 wt.%).

The SEM micrograph of PMMA1/70E-*gr*-*pl*PHEA (35.3%) after extraction with boiling water at 100 °C for 10 days and dried in vacuo afterwards is shown in Fig. 3.

3.3. Fourier transform infrared spectroscopy (FTIR)

No significant differences in the FTIR spectra of PMMA1/70E before and after plasma treatment were detected (results not shown).

Fig. 4 shows the FTIR spectra of the surface and cross-section of PMMA1/70E-*gr*-*pl*PHEA (35.3%). The spectra are nearly identical and the result proves that the *pl*PHEA coating is formed not only at the skin but also in the core of the macroporous PMMA samples. The FTIR spectra of the cross-section and the surface show the same adsorption peaks with similar intensity: a broad absorption peak around 3400 cm^{-1} due to the OH stretching vibration, the CH_2 and CH_3 stretching vibrations in the region of 2800–3000 cm^{-1}, the stretching of the carbonyl group at 1724 cm^{-1} and the absorption bands characteristic of carboxylic acid esters at $\sim$1143 cm^{-1}.

The FTIR spectra of sample PMMA1/70E-*gr*-*pl*PHEA (35.3%) after extraction with distilled water at 25 and 50 °C do not suffer chemical modifications. However, a strong change is produced after extraction at 100 °C for 10 days (see Fig. 5).

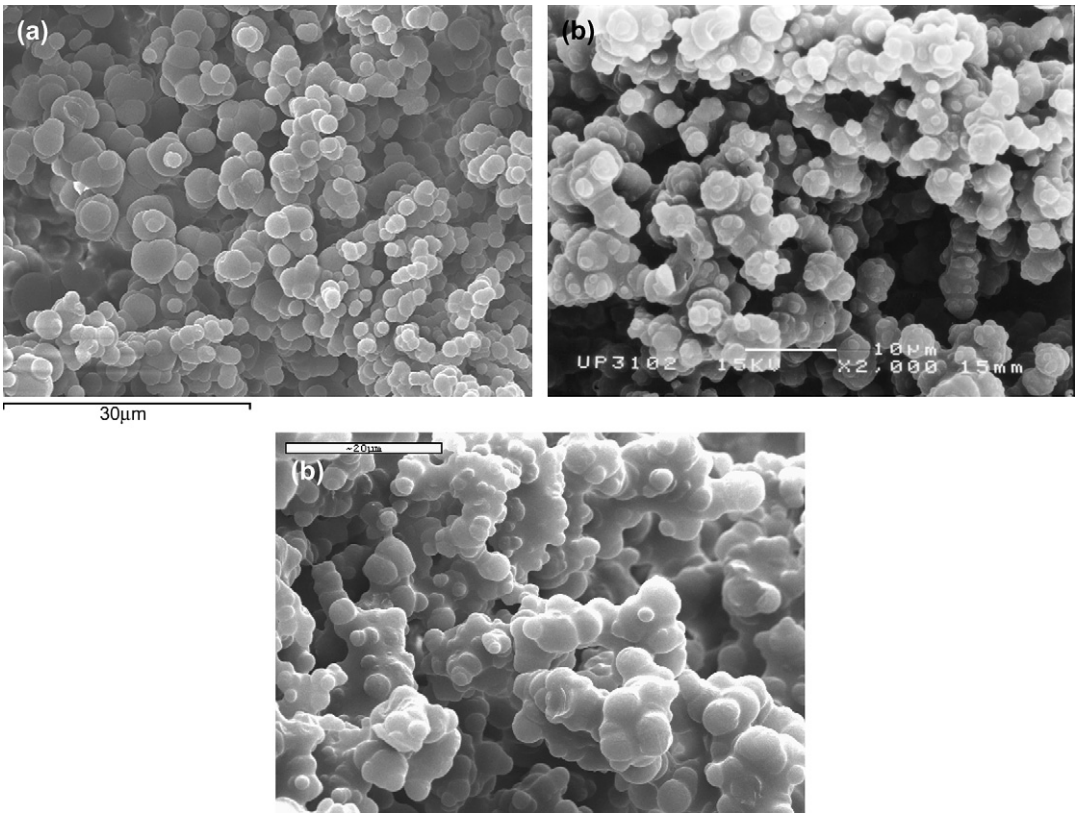

Fig. 2. SEM micrographs of PMMA5/70E with different wt.% of *pl*PHEA (0 (a), 25.3 (b) and 55.2 (c)) obtained by controlling adsorption time (0, 40 and 360 h, respectively). All micrographs have the same magnification (2000×).

The broad absorption around 3423 cm^{-1} due to the OH stretching vibration present in the *pl*PHEA polymer almost disappears and the strong band due to the presence of the carbonyl group at 1724 cm^{-1} loses its typical strong intensity. Besides, the CH_2 and CH_3 stretching vibrations in the region of 2800–3000 cm^{-1}, the absorption band characteristic of carboxylic acid esters at 1167 cm^{-1} and the stretching band of the alcohol group (C–O) suffer strange modifications become almost negligible.

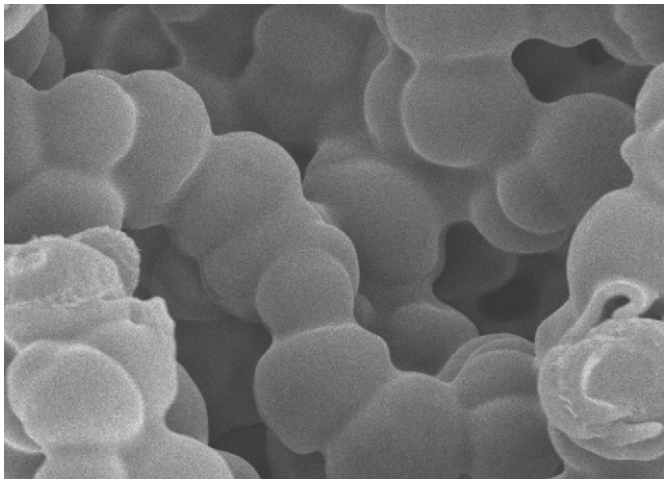

Fig. 3. SEM micrograph (4000×) of PMMA1/70E-*gr*-*pl*PHEA (35.3%) after extraction with boiling water for 10 days and dried in vacuo afterwards.

3.4. Stability of the plPHEA coating

The weight loss after extraction with water at 25 and 50 °C is practically negligible (results not shown). However, after extraction at 100 °C a significant weight loss is observed (see Table 2). Although, the weight losses of these PMMA-*gr*-*pl*PHEA samples are always much smaller than the weight fraction of *pl*PHEA present in the samples.

The DSC thermograms of sample PMMA1/70E-*gr*-*pl*PHEA (35.3%) before and after extraction with distilled

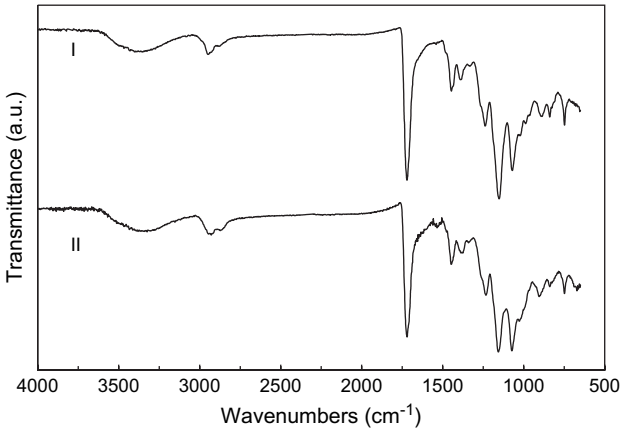

Fig. 4. FTIR spectra of the surface (I) and the cross-section (II) of PMMA1/70E-*gr*-*pl*PHEA (35.3%).

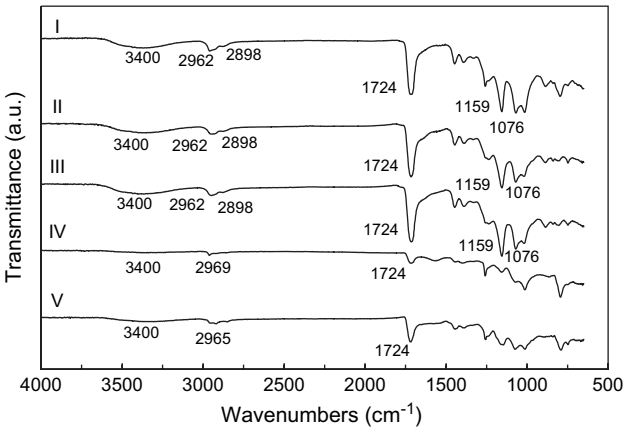

Fig. 5. FTIR spectra of sample PMMA1/70E-*gr*-*pl*PHEA (35.3%) before (I) and after extraction with distilled water at 25 (II), 50 (III) and 100 °C (surface (IV) and cross-section (V)) for 10 days and dried in vacuo afterwards.

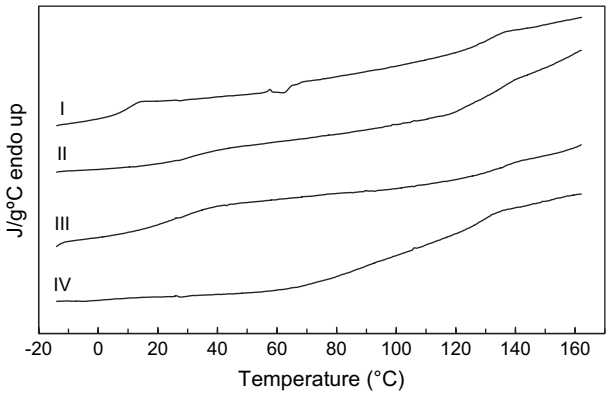

Fig. 6. DSC thermograms of sample PMMA1/70E-*gr*-*pl*PHEA (35.3%) before (I) and after extraction with distilled water at 25 (II), 50 (III) and 100 °C (IV) for 10 days and dried in vacuo afterwards.

water at 25, 50 and 100 °C for 10 days and dried in vacuo afterwards are shown in Fig. 6.

3.5. Equilibrium water uptakes

The equilibrium water uptakes of macroporous PMMA, bulk PHEA, PMMA-*gr*-*pl*PHEA and the *pl*PHEA present in these composite materials at 50 °C and two relative humidities are shown in Table 3. After the plasma grafting, the water sorption properties of these materials increase very much. The water uptakes of *pl*PHEA present in two PMMA-*gr*-*pl*PHEA scaffolds were determined as gram of adsorbed water per gram of *pl*PHEA in the composite material. These results show significant differences due to the degree of interpenetration depending on the PMMA substrate.

4. Discussion

Before the plasma grafting, when macroporous PMMA is exposed to a monomer vapour atmosphere, the substrate adsorbs HEA vapour. Diffusion of the monomer into the PMMA microspheres is a slow process since the PMMA network is in the glassy state at the temperature of the sorption process. Fig. 7 shows the continuous increase of the monomer absorbed by the substrate up to 360 h in the monomer atmosphere. The adsorption of the monomer molecules on the surface of the substrate is expected to be a fast process while the diffusion of HEA inside the substrate needs the plasticization of the polymeric substrate by the HEA absorbed and the propagation of the interface between plasticized and unplasticized PMMA towards the centre of the microspheres. The slow increase of HEA content in the PMMA scaffolds proves that HEA swells the PMMA network at least in the proximity of the surface. Plasma-induced polymerisation of HEA monomer produces a layer of *pl*PHEA what is expected to form a polymer network that in some extent interpenetrates the PMMA network of the substrate. The SEM micrographs of PMMA1/70E and PMMA1/70E-*gr*-*pl*PHEA (18.2%) were analysed measuring 50 microsphere diameters in order to have an estimation of the increase of the PMMA microsphere diameter after the polymerisation. The mean diameter of the observed microspheres increases from 4 ± 1 μm in the uncoated scaffold to 9 ± 2 μm in PMMA1/70E-*gr*-*pl*PHEA (18.2%). Fig. 8 shows, apart to the shift to larger diameters, the broadening of the distribution of the particle sizes with coating. The microsphere diameter of sample PMMA1/70E-*gr*-*pl*PHEA (18.2%) is more than two times larger than that of PMMA1/70E. Therefore, the *pl*PHEA layer formed onto the macroporous PMMA structure after the polymerisation is approximately 2.5 μm thick for sample PMMA1/70E-*gr*-*pl*PHEA (18.2%). For a higher amount of *pl*PHEA, it is not possible to measure the microsphere diameter because all the PMMA microspheres get covered with the *pl*PHEA coating without keeping their spherical shape. These hydrophilic coating penetrates the whole volume of the scaffold according to the FTIR results (Fig. 4). This proves that *pl*PHEA polymerisation can be initiated by plasma at any point of the porous structure of macroporous PMMA.

Table 2
Weight percent of weight loss of the PMMA-*gr*-*pl*PHEA samples after 10 days of extraction with boiling water and dried in vacuo afterwards

Sample	Weight loss at 100 °C (%)
PMMA1/70E-*gr*-*pl*PHEA (11.4%)	9.7
PMMA1/70E-*gr*-*pl*PHEA (24.8%)	6.4
PMMA1/70E-*gr*-*pl*PHEA (35.3%)	3.7
PMMA5/70E-*gr*-*pl*PHEA (25.3%)	2.7

Table 3
Equilibrium water uptakes ($w = m_{water}/m_{drypolymer}$) of bulk PHEA, *pl*PHEA and macroporous PMMA with different solvent, cross-linker and *pl*PHEA contents at 50 °C and two relative humidities (rh = 50.93 and 95.82%)

Sample	w (rh = 50.93%)	w (rh = 95.82%)
PMMA1/70E	0.00388	0.01189
PMMA5/70E	0.00507	0.01298
*PMMA1/70E-gr-*pl*PHEA (18.2%)	0.00832	0.04247
**PMMA5/70E-gr-*pl*PHEA (25.3%)	0.01009	0.02459
*pl*PHEA in *	0.04558	0.23339
*pl*PHEA in **	0.03989	0.09719
Bulk PHEA	0.07559	0.41424

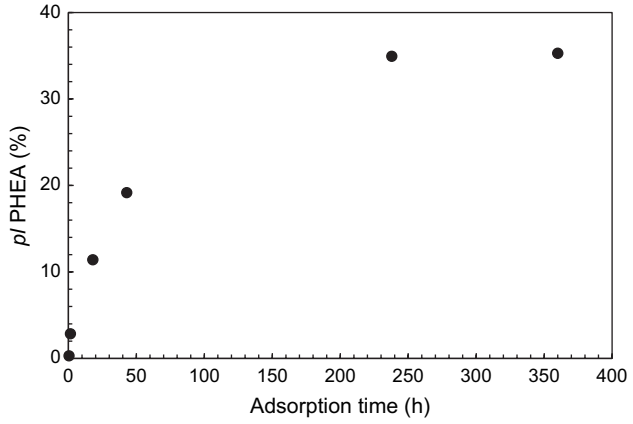

Fig. 7. Weight fraction (in %) of plasma-polymerised PHEA grafted onto macroporous PMMA1/70E as a function of adsorption time of the HEA monomer vapour before the plasma treatment.

Macroporous PMMA can be prepared with the desired amount of *pl*PHEA simply controlling adsorption time. A graph of the wt.% of *pl*PHEA obtained as a function of adsorption time of the HEA monomer vapour before the plasma treatment is shown in Fig. 7. After a certain adsorption time, approximately 250 h, the effect of adsorption time is attenuated because the PMMA network gets saturated of HEA vapour reaching the thermodynamical equilibrium.

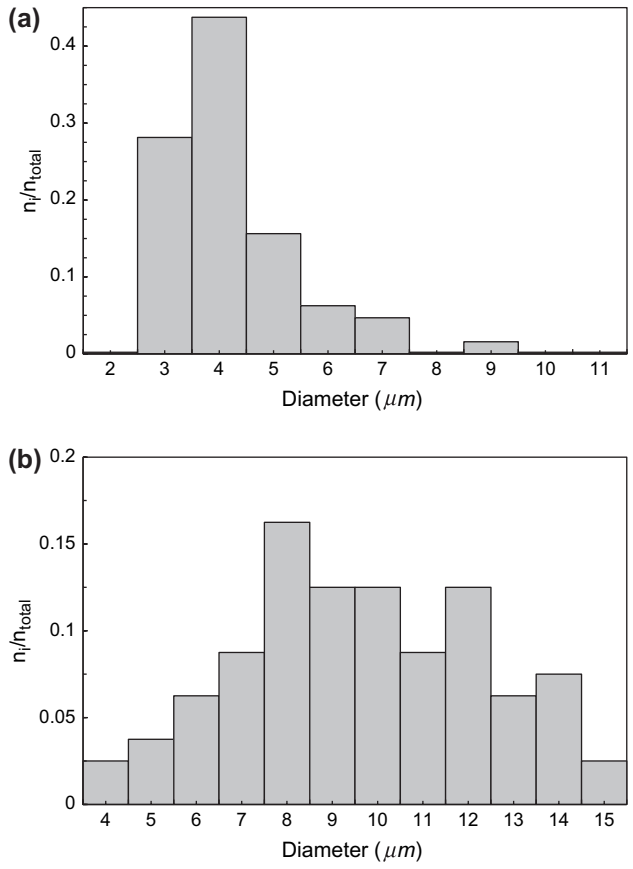

Fig. 8. Microsphere diameter distribution bar graph of PMMA1/70E (a) and PMMA1/70E-*gr*-*pl*PHEA (18.2%) (b).

The adsorption of HEA is much faster on the substrate PMMA5/70E than in PMMA1/70E. Almost double amount of *pl*PHEA was obtained in PMMA5/70E (55.2 wt.%) than in PMMA1/70E (35.3 wt.%) for the same adsorption time (360 h). One of the reasons for that behaviour is the higher porosity of PMMA5/70E (see Table 1), what means more specific area available for HEA vapour adsorption. In addition, the polarity of PMMA increases with increasing the EGDMA content, what favours the swelling of the PMMA microspheres.

Since the plasma treatment takes place only on the surface of the PMMA microspheres with adsorbed HEA monomer, the PMMA-*gr*-*pl*PHEA microspheres obtained after the polymerisation are expected to consist of a pure PMMA nucleus, a *pl*PHEA–PMMA interpenetrated polymer layer (IPN) and a pure *pl*PHEA layer on the surface. The plasma treatment let the HEA monomer polymerise on the surface and only some radicals could achieve to polymerise inside the PMMA network as an IPN. Table 1 shows that the porosities of macroporous PMMA polymerised with 1 wt.% of EGDMA decrease very much after the polymerisation. However, almost no change was found in the case of the scaffolds polymerised with 5 wt.% cross-linker. This means that in PMMA1/70E-*gr*-*pl*PHEA most of the *pl*PHEA is on the surface occupying a part of the volume of pores existing in the uncoated porous sample while the *pl*PHEA is more homogeneously interpenetrated in the scaffold with a higher amount of cross-linker. If the SEM micrographs shown in Figs. 1 and 2 are analysed, the PMMA microspheres coated with *pl*PHEA keep better their shape in PMMA1/70E than in PMMA5/70E. These SEM micrographs of PMMA5/70E with different *pl*PHEA contents show that the PMMA microsphere shapes are very irregular after the polymerisation.

When *pl*PHEA is grafted onto macroporous PMMA, water sorption considerably increases, especially for high relative humidity. Table 3 shows smaller water uptakes for *pl*PHEA than bulk PHEA. For high relative humidities, these differences are even larger because the hydrophobic substrate impedes the expansion of the *pl*PHEA network. The *pl*PHEA present in the macroporous substrate with higher cross-linker density shows the smallest water uptakes because this *pl*PHEA is more homogeneously interpenetrated.

Table 2 shows significant weight losses after extraction with water at 100 °C. Part of this weight loss can be due to a small fraction of the PMMA microspheres that are not enough joined to resist the strong push of water when filling the pores with water. This explains the fact that the PMMA-*gr*-*pl*PHEA samples with less *pl*PHEA has the highest weight loss probably because the adhesion between PMMA particles in these samples is poorer than in the rest. Nevertheless, sample 5/70E-*gr*-*pl*PHEA (25.3%) has the lowest weight loss showing that the *pl*PHEA is more homogeneously interpenetrated in this sample because there is more cross-linker.

On the other hand, after extraction at 25 and 50 °C the glass transition of the *pl*PHEA coating is observed by DSC (Fig. 6) and the FTIR spectrum before and after extraction at these temperatures does not show any chemical change. Nevertheless the FTIR spectra of the samples immersed in boiling

water show clear differences with respect to the untreated sample that can be indicative of hydrolytic degradation (see Fig. 5). Hydrolysis mechanisms are the most important degradation reactions involving ester groups in the backbone or the side chain of polymeric materials, which revert to the carboxylic acid and alcohol [20]. These results, weight losses and chemical changes, can be explained by the loss of side-chain $CO-O-CH_2CH_2OH$ groups by hydrolytic degradation. The effect of the water extraction on the surface of the sample seems to be more important than in the core of the scaffold as shown by the FTIR spectra of the surface and cross-section of the samples (Fig. 5). This is also in good agreement with the DSC results where the glass transition of *pl*PHEA disappears after extraction at 100 °C (see Fig. 6). Nevertheless, the plasma-polymerised hydrophilic coating can be observed by SEM even after suffering such drastic changes in its physical and chemical properties (see Fig. 3).

From these results, it can be concluded that the *pl*PHEA coating is very stable, it cannot be dissolved in water and must be cross-linked to some extent.

5. Conclusions

Poly(2-hydroxyethyl acrylate) hydrophilic coatings can be grafted onto macroporous poly(methyl methacrylate) by adsorbing monomer vapour and subsequent plasma-induced polymerisation without the need of thermal or photoinitiators. The amount of grafted *pl*PHEA can be controlled with the sorption time of HEA vapour. A homogeneous coating is formed around all the PMMA microspheres inside and on the surface of macroporous PMMA according to the FTIR measurements. This plasma-polymerised PHEA coating is pure because it is obtained after adsorbing HEA monomer vapour. The plasma-polymerised PHEA cannot be dissolved in water probably because it is cross-linked to some extent and interpenetrated. It is chemically very stable and only in very drastic conditions (immersion in boiling water for 10 days) it suffers hydrolytic degradation. The formation of the hydrophilic coating can be clearly observed by scanning electron microscopy.

The *pl*PHEA coating is more homogeneously interpenetrated with macroporous PMMA polymerised with 5 wt.% of EGDMA because there is more cross-linker. The *pl*PHEA grafted onto macroporous PMMA with 1 wt.% of EGDMA is less homogeneously interpenetrated (mostly on the surface of the PMMA microspheres). Thus, the porosity of macroporous PMMA polymerised with 1 wt.% of EGDMA decreases after polymerisation and hardly changes in macroporous PMMA with 5 wt.% of EGDMA.

By means of this particular protocol of plasma-induced polymerisation it is possible to graft hydrophilic polymers onto hydrophobic scaffolds keeping their initial porosity. This composite material can form a resistant polymer hydrogel when water is absorbed.

Acknowledgement

This work was supported by the Spanish Science and Technology Ministry through the MAT2002-04239-C03-03 project.

References

[1] Soichet MS, Hubbell JA. Polymers for tissue engineering. Utrecht: VPS; 1998.
[2] Dimitriu S, editor. Polymeric biomaterials. New York: Marcel Dekker; 1994.
[3] Vallet Regi M, Munera L, editors. Biomateriales aquí y ahora. Madrid: Dykinson; 2000.
[4] Tanzawa H, Nagaoka S, Suzuki J, Kobayashi S, Masubuchi Y, Kikuchi T. Cell adhesion and growth on the surface of synthetic hydrogels. In: Goldberg E, Nakajima A, editors. Biomedical polymers. New York: Academic Press; 1980. p. 189–211.
[5] Brígido Diego R, Pérez Olmedilla M, Serrano Aroca A, Gómez Ribelles JL, Monleón Pradas M, Gallego Ferrer G, et al. J Mater Sci Mater Med 2005;16:693.
[6] Safinia L, Datan N, Höhse M, Mantalaris A, Bismarck A. Biomaterials 2005;26:7537.
[7] Inagaki N. Plasma surface modification and plasma polymerisation. Technomic Publishing Company, Inc.; 1996.
[8] Lieberman MA, Lichtenberg AJ. Principles of plasma discharges and materials processing. John Wiley & Sons, Inc.; 1994.
[9] Zhang C, Wyatt J, Russell SP, Weinkauf DH. Polymer 2004;45:7655.
[10] Russell SP, Weinkauf DH. Polymer 2001;42:2827.
[11] Denes F, Sarmadi AM, Hop CECA, Young RA. J Appl Polym Sci Appl Polym Symp 1994;54:55.
[12] Gaur S, Vergason G. 43rd Annual Technical Conference Proceedings. Denver; April 15–20, 2000.
[13] Lin Y, Yasuda H. J Appl Polym Sci 1996;60:543.
[14] Yashuda H. Plasma polymerization. Orlando: Academic Press; 1985.
[15] Petasch W, Räuchle E, Weichart J, Bickmann H. Surf Coat Technol 1995;74–75(1–3):200–5.
[16] Greenspan L. J Res Natl Bur Stand, US, 1997;81:89.
[17] Dušek KJ. Polym Sci C 1967;16:1289.
[18] Dušek K. In: Chompff AJ, Newman S, editors. Polymer networks—structure and mechanical properties. New York: Plenum Press; 1971.
[19] Serrano Aroca A, Monleón Pradas M, Gómez Ribelles JL. Coll Polym Sci, in press.
[20] Amass W, Amass A, Tighe B. Polym Int 1998;47:89.